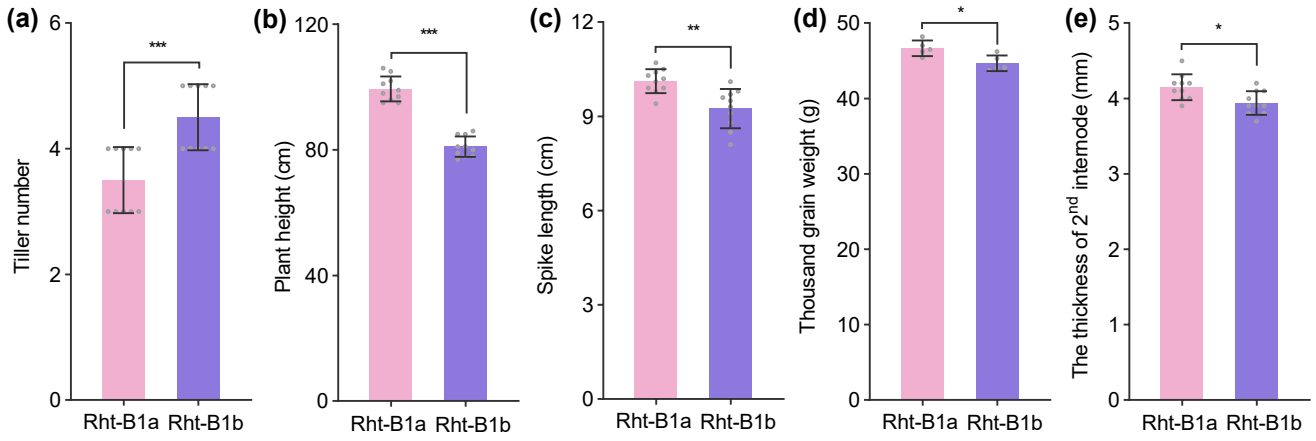

Figure S1 The genetic effect of the wheat Green Revolution gene *Rht-B1b* that reduced plant height but produced smaller spikes. Statistical analysis of tiller number (a), plant height (b), spike length (c), thousand grain weight (d), and the thickness of 2nd internode (e) of the *Rht-B1a* and *Rht1* mutant (*Rht-B1b*). Data were presented as mean ± s.d.; *P* values were determined by two-tailed Student's *t*-test. **P*< 0.05, ***P*< 0.01, ****P*< 0.001.

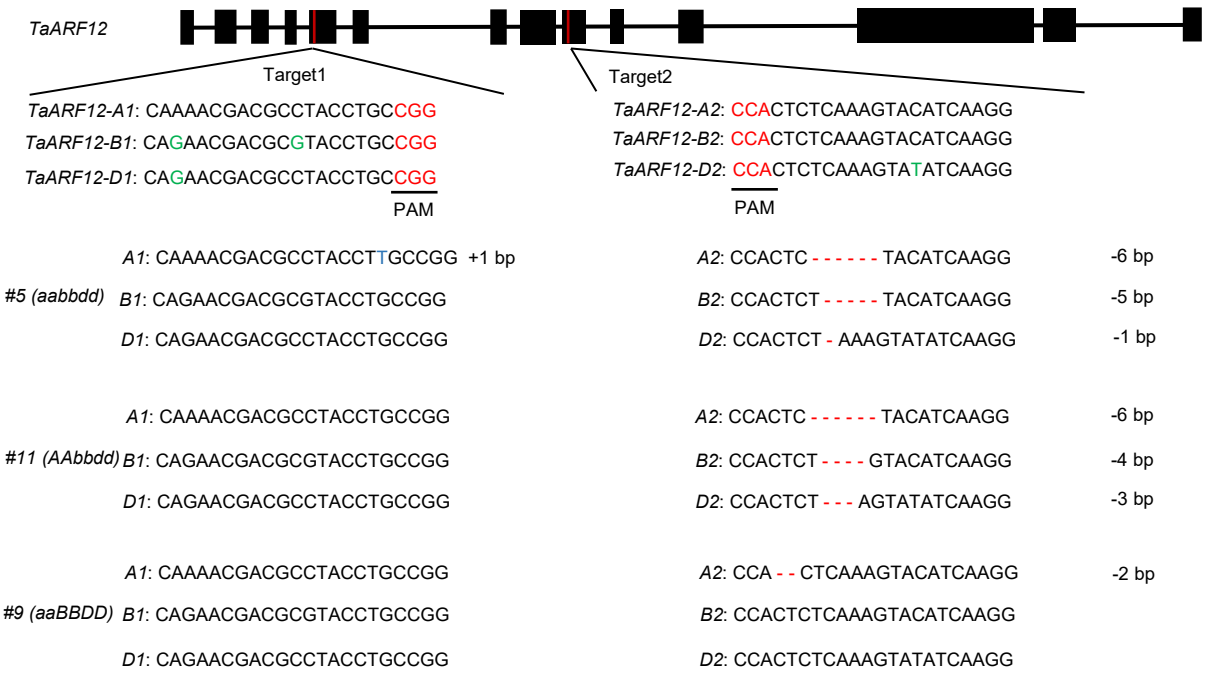

Figure S2 CRISPR/Cas9 mediated mutagenesis of *TaARF12*. Two guide RNAs (sgRNA) were designed to target all three homoeologs that may cause early stop codon during translation. All three homoeologs were targeted at the right sgRNA (target 2) for lines #5 and #11 while only one homoeolog was edited for line #9. Only one homoeolog was targeted at the left sgRNA (target 1) for line #5. PAM sequences are underlined and highlighted in red. Insertion is highlighted in blue. The deleted nucleotides in edited plants are indicated by red dashes.

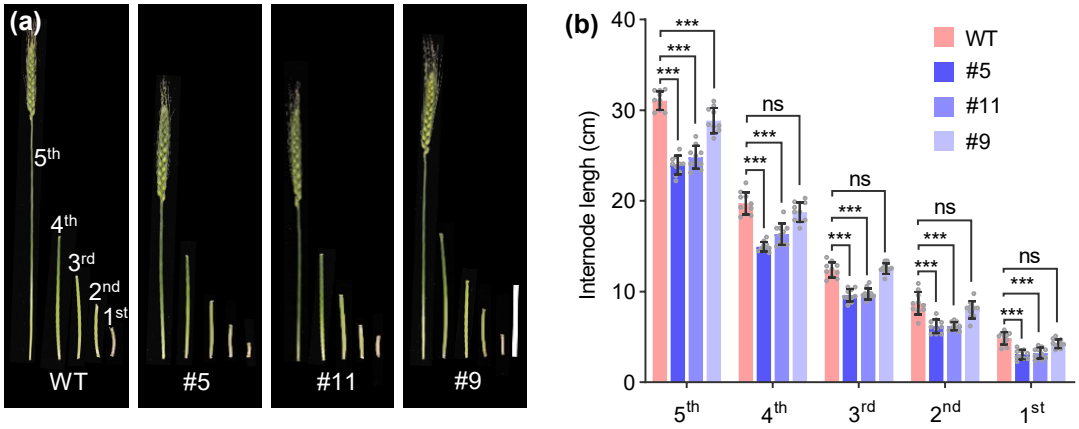

Figure S3 Morphological comparison of stem internodes of the wild type and t*aarf12* transgenic lines. (a) Stem internodes of a main tiller of the wild type (WT) Fielder and three *taarf12* transgenic plants showing shorter internode in the latter. Scale bar, 10 cm. (b) Statistical analysis of internode lengths of WT and *taarf12* plants. Data were presented as mean ± s.d.; *P* values were determined by two-tailed Student's *t*-test. ***$P < 0.001$; ns, not significant.

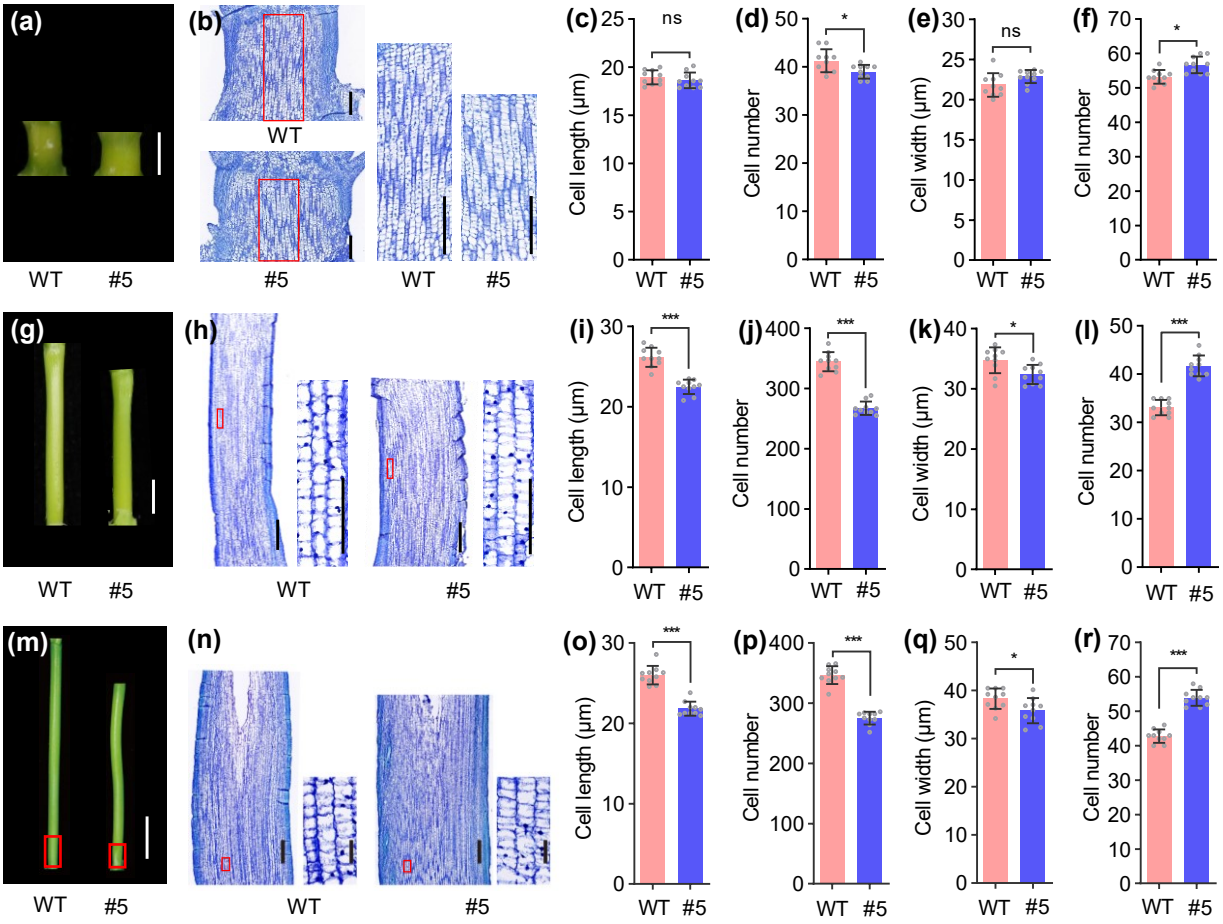

Figure S4 Longitudinal dissection illustrated that *taarf12* peduncles were shorter with fewer cells that may be responsible for reduced peduncle length while more cell layers presented in stem may make it stronger. (a, g, m) Peduncles of the wild type (WT) and *taarf12* at developmental stages W7.0 (a), W8.5 (g), and W9.0 (m). Scale bars, 1 mm (a), 2 mm (g), 1 cm (m). (b, h, n) Longitudinal sections of peduncles at W7.0 (b), W8.5 (h) and W9.0 (n). Longitudinal sections in (n) corresponded to the red rectangles in (m). Scale bars, 200 μm (b), 1 mm for the whole internode section and 200 μm for the enlarged picture of red rectangle in (h), 500 μm for the whole internode section and 50 μm for the enlarged picture of the red rectangle in (n). (c, d, i, j, o, p) Statistical analyses of longitudinal cell length (c, i, o) and cell number (d, j, p) of peduncles of WT and *taarf12* plants at W7.0 (c, d), W8.5 (i, j) and W9.0 (o, p) stages. (e, f, k, l, q, r) Statistical analysis of horizontal cell width (e, k, q) and cell number (f, l, r) of peduncles at stages W7.0 (e, f), W8.5 (k, l), and W9.0 (q, r). Data were presented as mean ± s.d.; *P* values were determined by two-tailed Student's *t*-test. **P*< 0.05; ****P*< 0.001; ns, not significant.

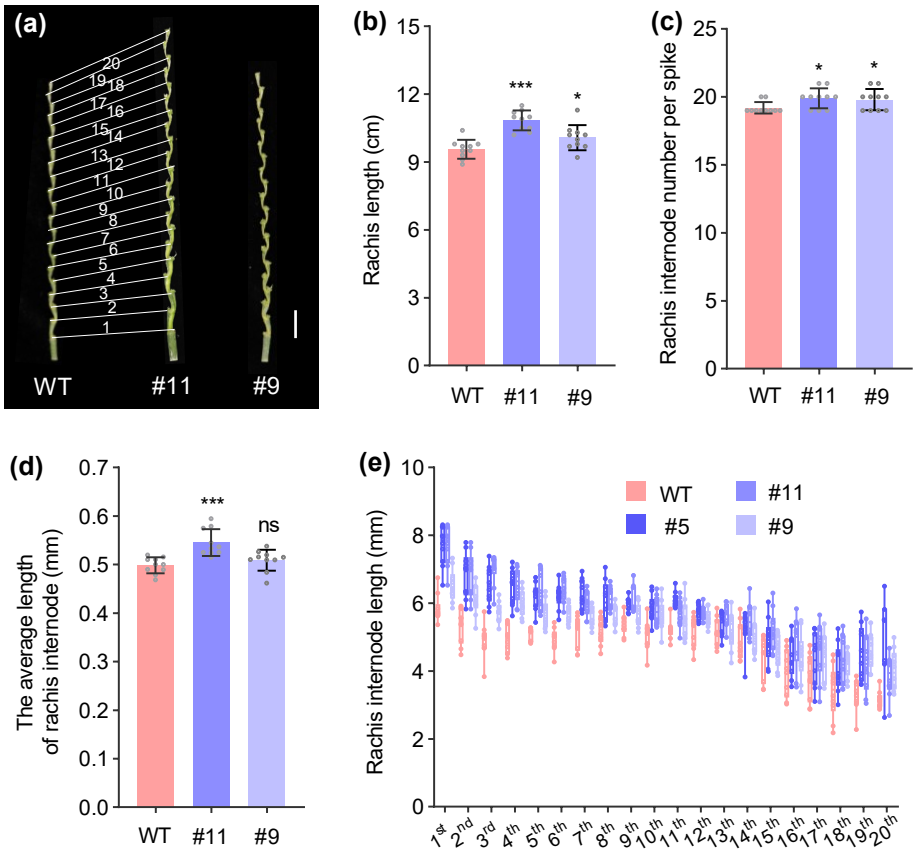

Figure S5 Comparison of the wild type and *taarf12* plants showed that the longer spikes in the latter were caused by rachis internode elongation. (a) Rachis and rachis internodes. Scale bar, 1 cm. (b-e) Statistical analyses of rachis length (b), rachis internode number per spike (c), the average length of rachis internode (d) and rachis internode length (e). Data were presented as mean ± s.d.; *P* values were determined by two-tailed Student's *t*-test. **P*< 0.05; ****P*< 0.001; ns, not significant.

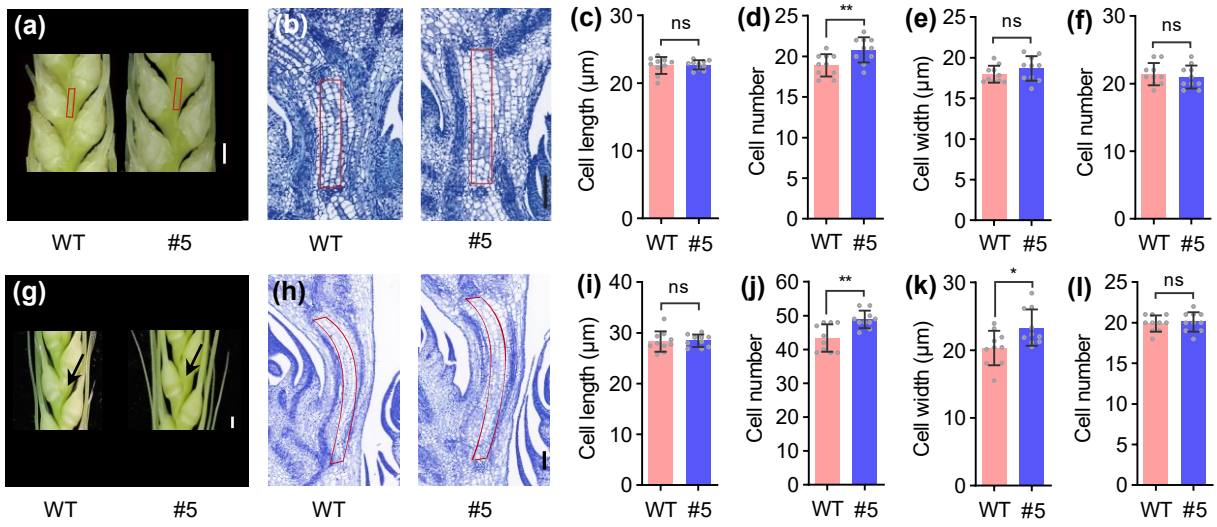

Figure S6 Longitudinal dissection of *taarf12* rachis demonstrates that the enlarged rachis was caused by increased cell number and cell size relative to that of the wild type. (a-f) Portions of spikes (a) and their sections at W5.5 (b) with statistics for longitudinal cell length (c), cell number (d), and horizontal cell width (e) and cell number (f). (g-l) Portions of spikes (g) and their sections at W7.5 (h) with statistics for longitudinal cell length (i), cell number (j), and horizontal cell width (k) and cell number (l). Scale bars, 500 μm (a, g) 100 μm (b, h). Data were presented as mean ± s.d.; *P* values were determined by two-tailed Student's *t*-test. **P*< 0.05; ***P*< 0.01; ns, not significant.

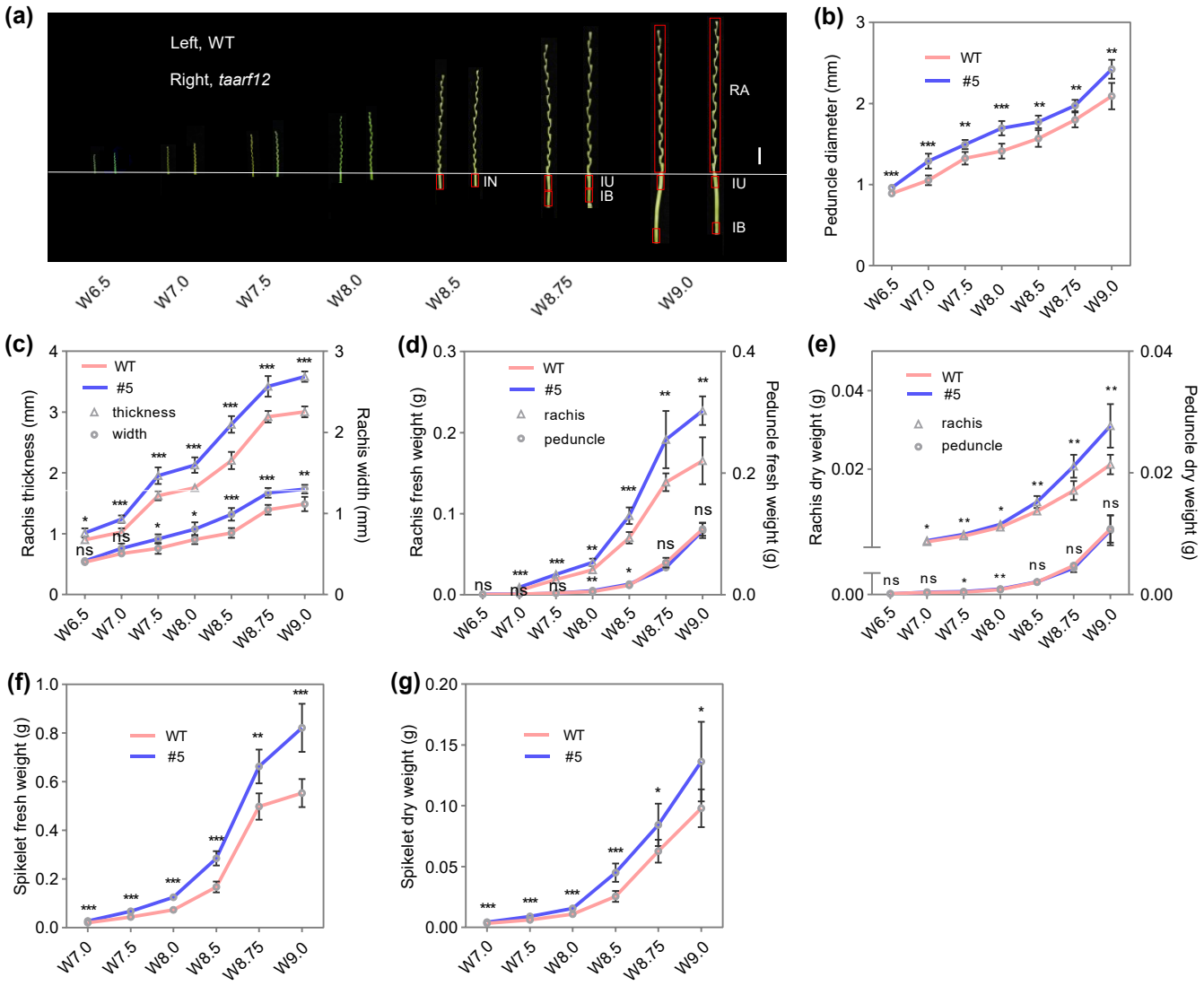

Figure S7 Phenotypic comparison of wild type and *taarf12* peduncle and rachis during their development. (a) Rachises with peduncles of WT and *taarf12* plants at various developmental stages indicated. Scale bar, 1 cm. IB, internode bottom portion; IN, internode/peduncle; IU, internode upper portion; RA, rachis. (b, c) Comparative statistics of peduncle diameter (b), rachis width and thickness (c) showing that thicker peduncle, and wider, and thicker rachis at indicated developing stages in *taarf12* plants. (d-g) Comparison of peduncle and rachis fresh weight (d), dry weight (e), spikelet fresh weight (f), and spikelet dry weight (g), showing heavier rachis and spikelet that may contribute to final harvest index. No significant changes occurred for peduncle. W, Waddington stages as described by Waddington et al., (1983); Data were presented as mean ± s.d.; *P* values were determined by two-tailed Student's *t*-test. **P*< 0.05; ***P*< 0.01; ****P*< 0.001; ns, not significant.

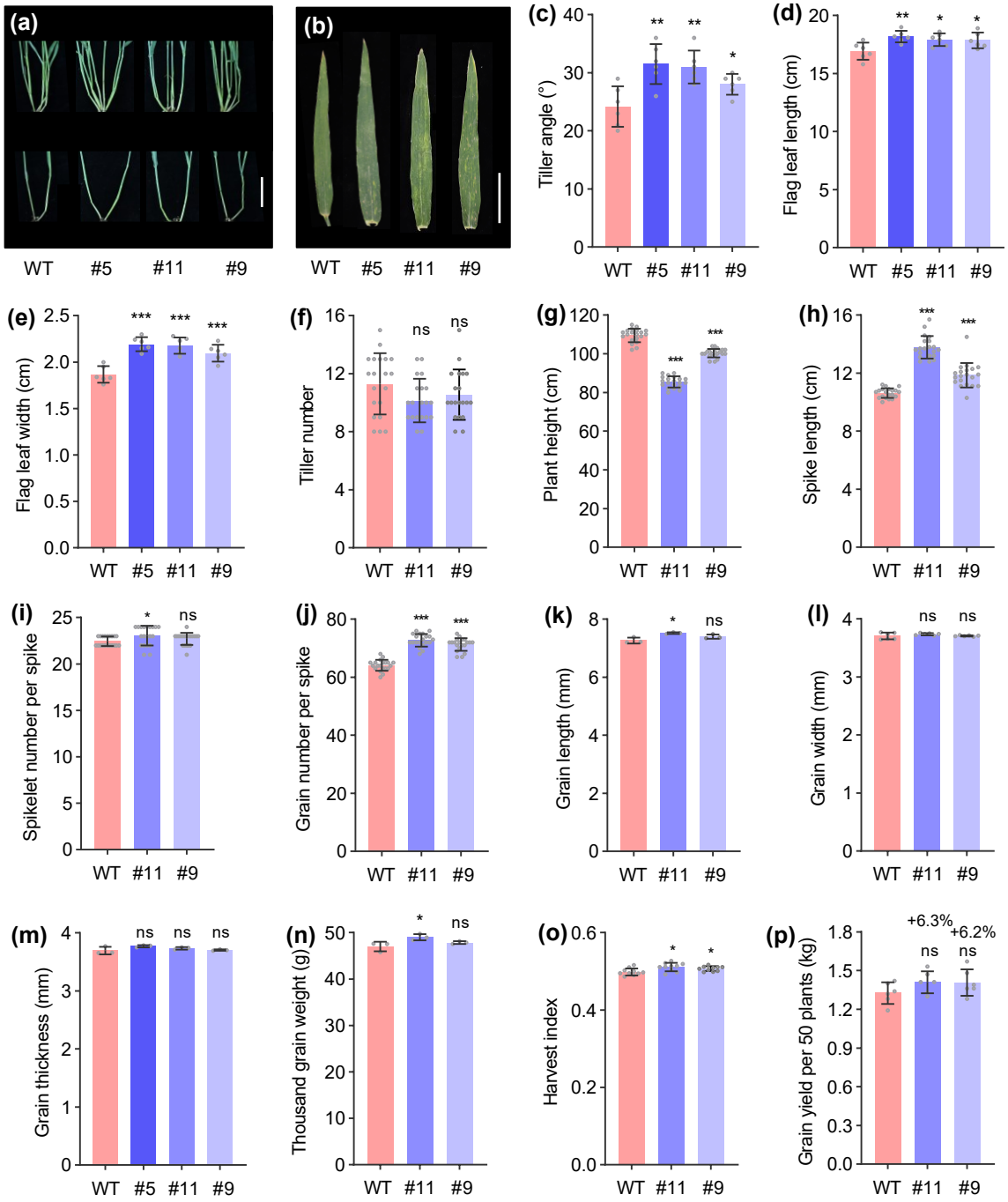

Figure S8 Statistics from field trials proved that the *taarf12* plants boosts grain yield. (a) The relative wider tiller angle of *taarf12* plants compared with those of the wild type (WT) Fielder. The tiller angle refers to the angle between the two outermost tillers. Scale bar, 10 cm. (b) *taarf12* flag leaves are longer and wider than those of WT. Scale bar, 5 cm. (c-p) Statistical analysis of tiller angle (c), flag leave length (d), flag leaves width (e), tiller number (f), plant height (g), spike length (h), spikelet number per spike (i), grain number per spike (j), grain length (k), grain width (l), grain thickness (m), thousand grain weight (n), harvest index (o), and grain yield per 50 plants (p). Wheat plants were grown in Hebei, China in October 2021. Data were presented as mean ± s.d.; *P* values were determined by two-tailed Student's *t*-test. **P*< 0.05; ***P*< 0.01; ****P*< 0.001; ns, not significant.

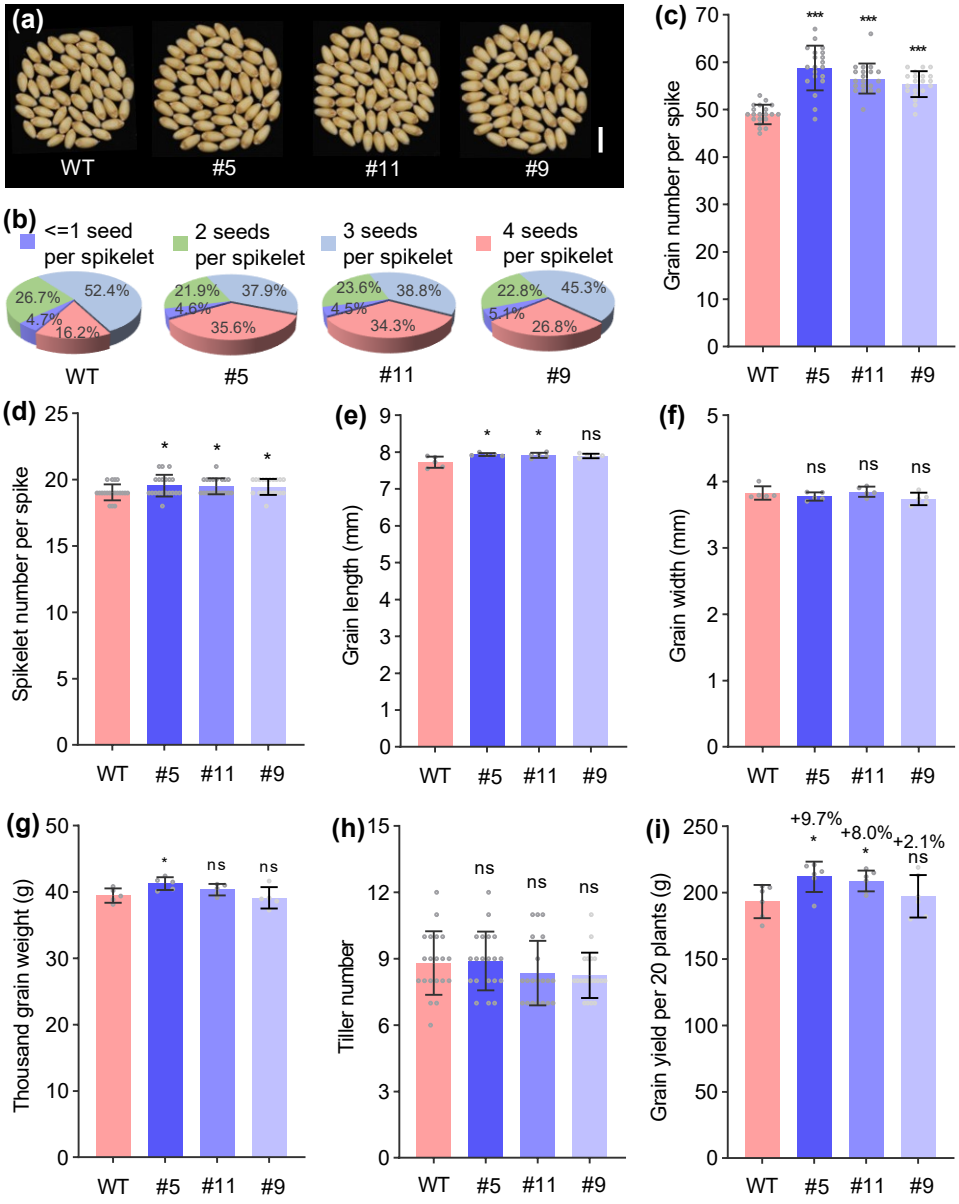

Figure S9 Grain traits from field plants revealed increased grain yield in *taarf12* plants. (a) Grains per spike of the wild type (WT) and three *taarf12* lines. Scale bar, 1 cm. (b) Percentages of spikelets with different grain numbers in the WT and *taarf12* plants. (c) Statistical analysis of grain number per spike exhibiting more grains in *taarf12* plants. (d-i) Statistical analysis of spikelet number per spike (d), grain length (e), grain width (f), thousand grain weight (g), tiller number (h), and grain yield per 20 plants (i) in WT and *taarf12* plants. Wheat plants were grown in Beijing, China in February 2020. Data were presented as mean ± s.d.; *P* values were determined by two-tailed Student's *t*-test. **P*< 0.05; ****P*< 0.001; ns, not significant.

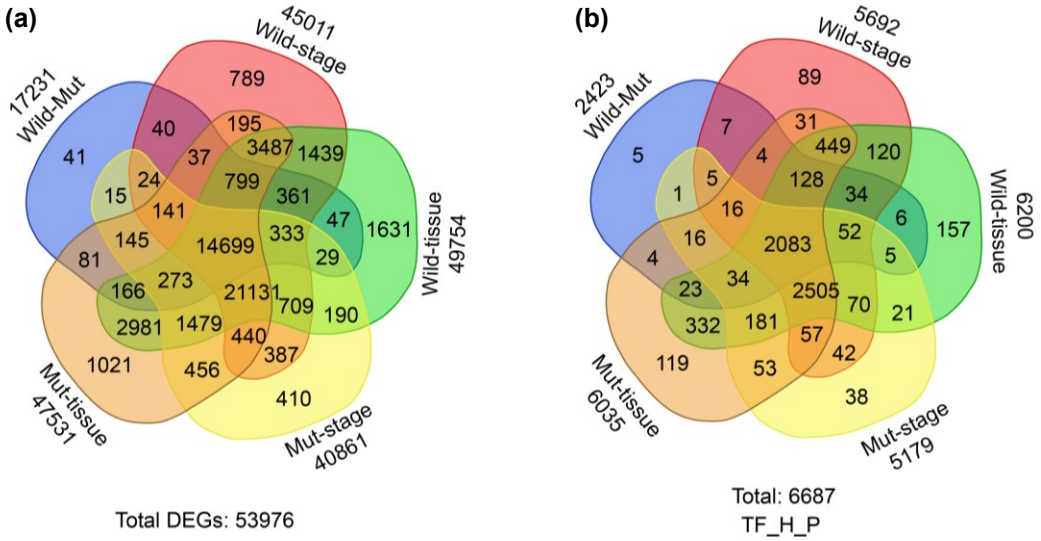

Figure S10 Venn diagrams showing DEGs shared by different spatial, temporal and tissue comparisons. (a) Venn diagram showing the sharing of all DEGs from various comparisons. (b) Venn diagram showing the sharing of selected DEGs encoding transcription factor- (TF), hormone- (H) and photosynthesis-related (P) as annotated by MapMan Bin. Wild-Mut represented DEGs between wild type Fielder and *taarf12* mutant. Wild-stage and Mut-stage represented development-affected DEGs of the wild type and *taarf12*, respectively. Wild-tissue and Mut-tissue represented DEGs from comparison of gene expression levels in corresponding tissues (IN, IB, IU, RA) of the wild type and *taarf12*, respectively.

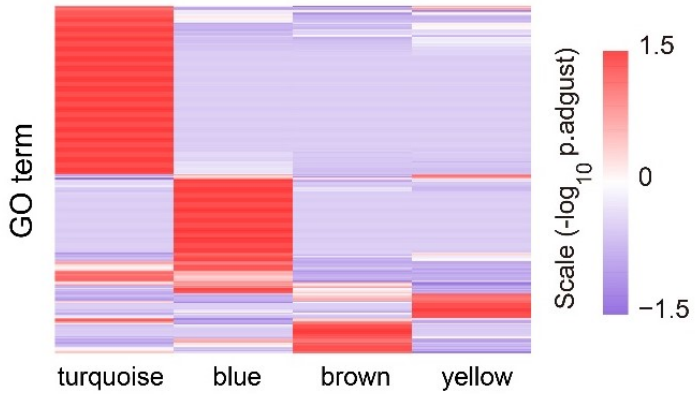

Figure S11 Heatmap of enriched Gene Ontology (GO) genes in each co-expression module of peduncle. Color intensity represents the significance scale (−log10[adjusted P value]) of GO term enrichment.

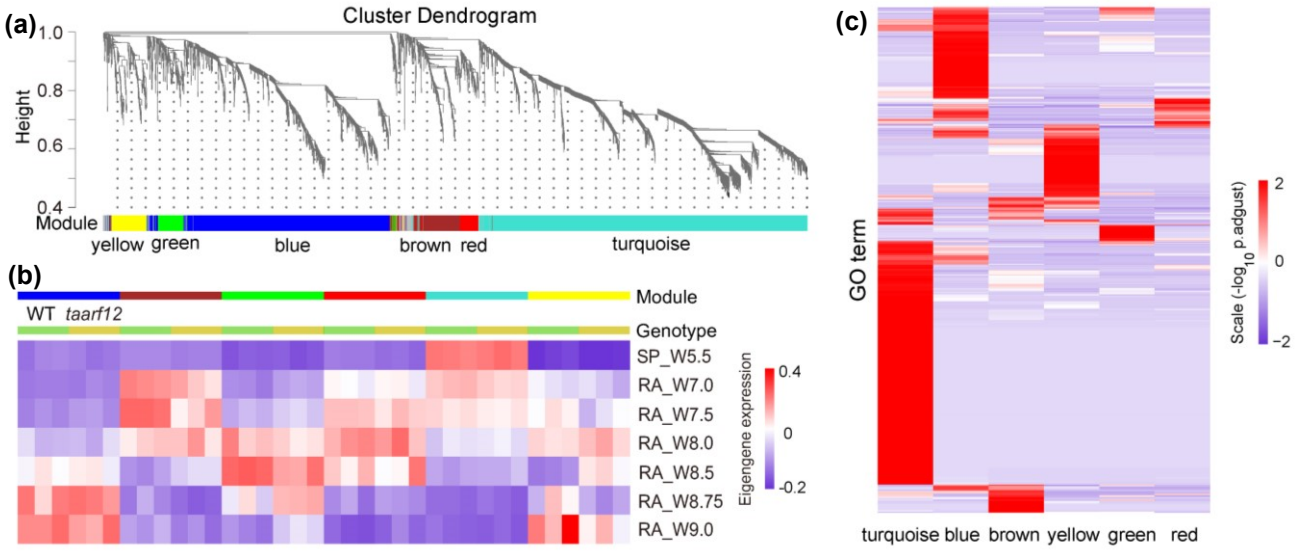

Figure S12 Gene co-expression modules of spike (SP) and rachis (RA) at W5.5-W9.0 of the wild type and *taarf12*. (a) Gene co-expression modules (CMs) generated using weighted gene co-expression network analysis (WGCNA) among spike and rachis. In the dendrogram, each leaf represents one gene, and each module below the dendrogram is labeled with one color. The threshold of hierarchical cluster dendrogram is the cut height (0.99) for CM identification. CM colors are labeled independent of the separately identified modules in each genotype. Genes not co-expressed in all three genotypes are marked in gray. (b) Differential eigengene expression patterns of CMs between wild type (WT) and *taarf12* in spike (W5.5) and rachis across W7.0–W9.0. Purple and red represent lesser and greater expression, respectively. (c) Heatmap of GO enrichment of genes in each CM. Color intensity represents the significance scale (−log10[adjusted *P* value]) of GO term enrichment.

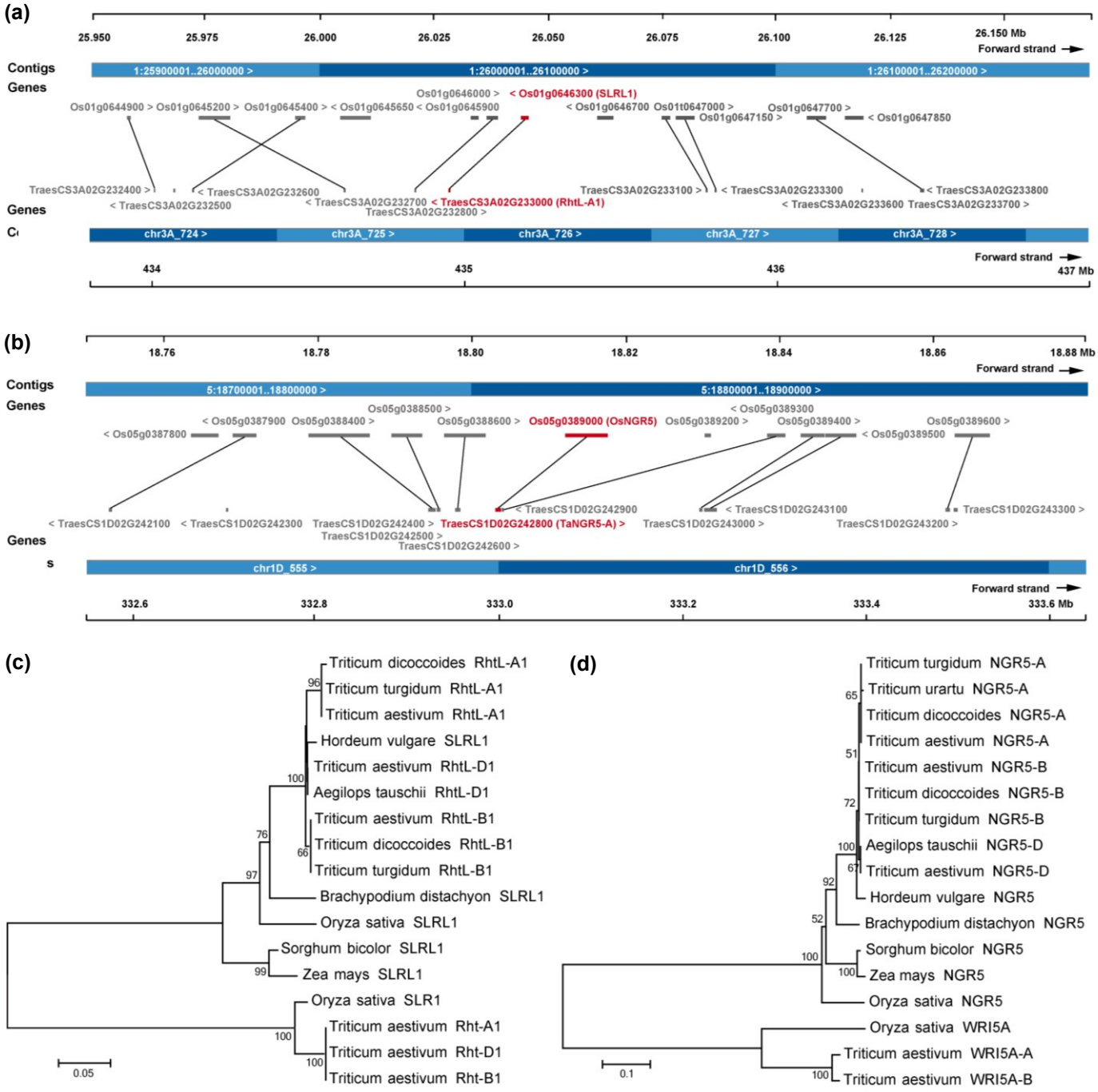

Figure S13 Rice-wheat genome collinearity at *RhtL1* and *TaNGR5* regions and phylogenetic trees of related genes from related species. (a, b) Collinear analyses of *RhtL1* (a) and *TaNGR5* (b) between wheat and rice genomes showing the ortholog of corresponding regions. The line connecting these pair genes indicates that they are orthologs between rice and wheat. (c, d) Neighbor joining trees of SLRL1 (c) and NGR5 (d) in monocotyledon. *Rht1* and *WRI5A* genes were used as outgroups. Bootstrap values of >50% is shown above branches.

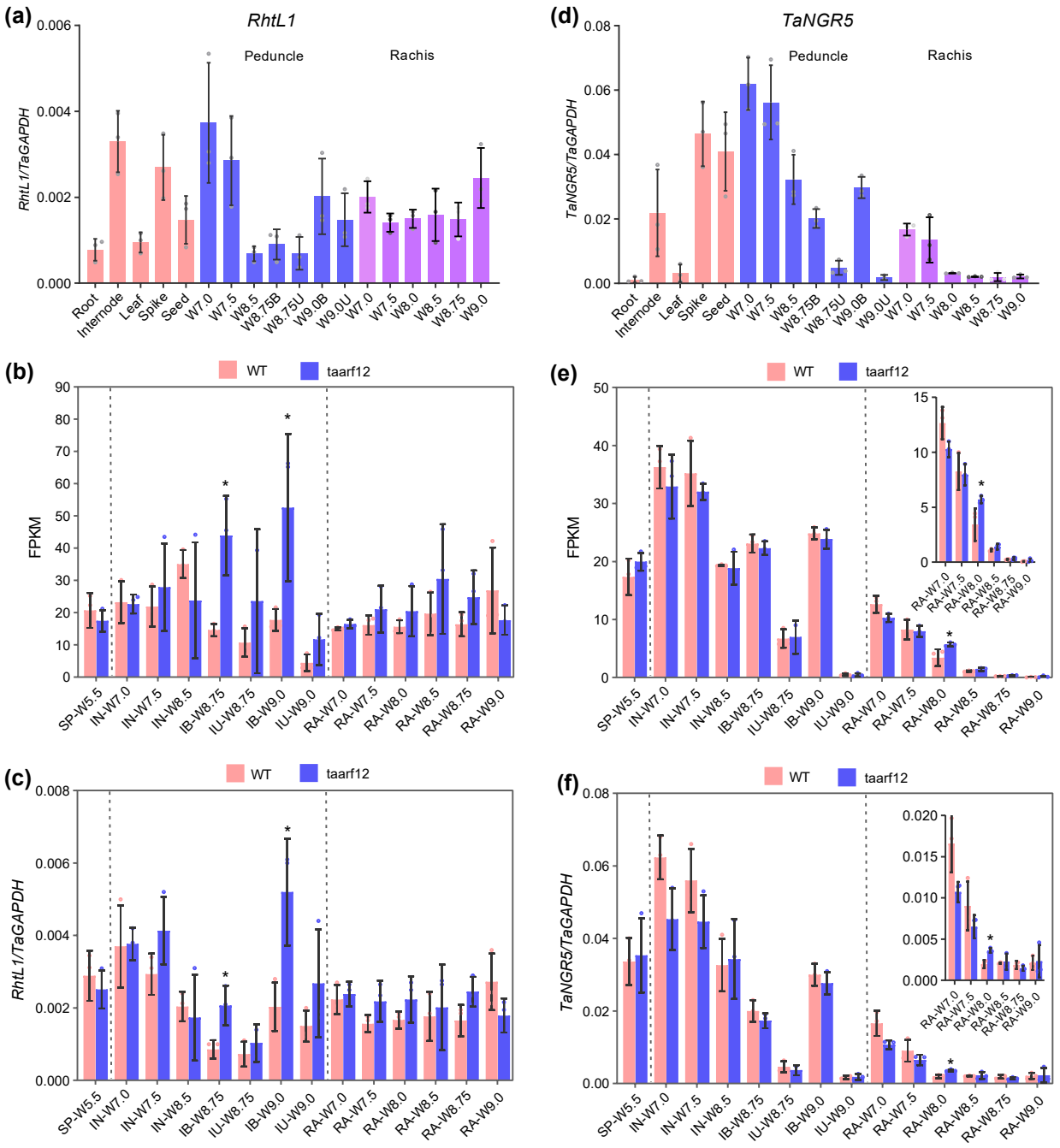

Figure S14 Spatial-temporal expression patterns of *RhtL1* and *TaNGR5* in wheat. (a, d) Relative expression levels of *RhtL1* (a) and *TaNGR5* (d） in different organs and developmental stages of peduncle, and rachis. W, Waddington stages as described by Waddington et al., (1983). (b, e) Relative expression of *RhtL1* (b) and *TaNGR5* (e) from RNA-seq data. (c, f) qRT-PCR confirmation of genes *RhtL1* (c) and *TaNGR5* (f) in wild type (WT) Fielder and *taarf12*. Insets in (e) and (f) are enlarged images of the low expression regions of the figure. IB, internode bottom portion; IN, internode/peduncle; IU, internode upper portion; RA, rachis; SP, spike. Data were presented as mean ± s.d.; *P* values were determined by two-tailed Student's *t*-test. **P*< 0.05.

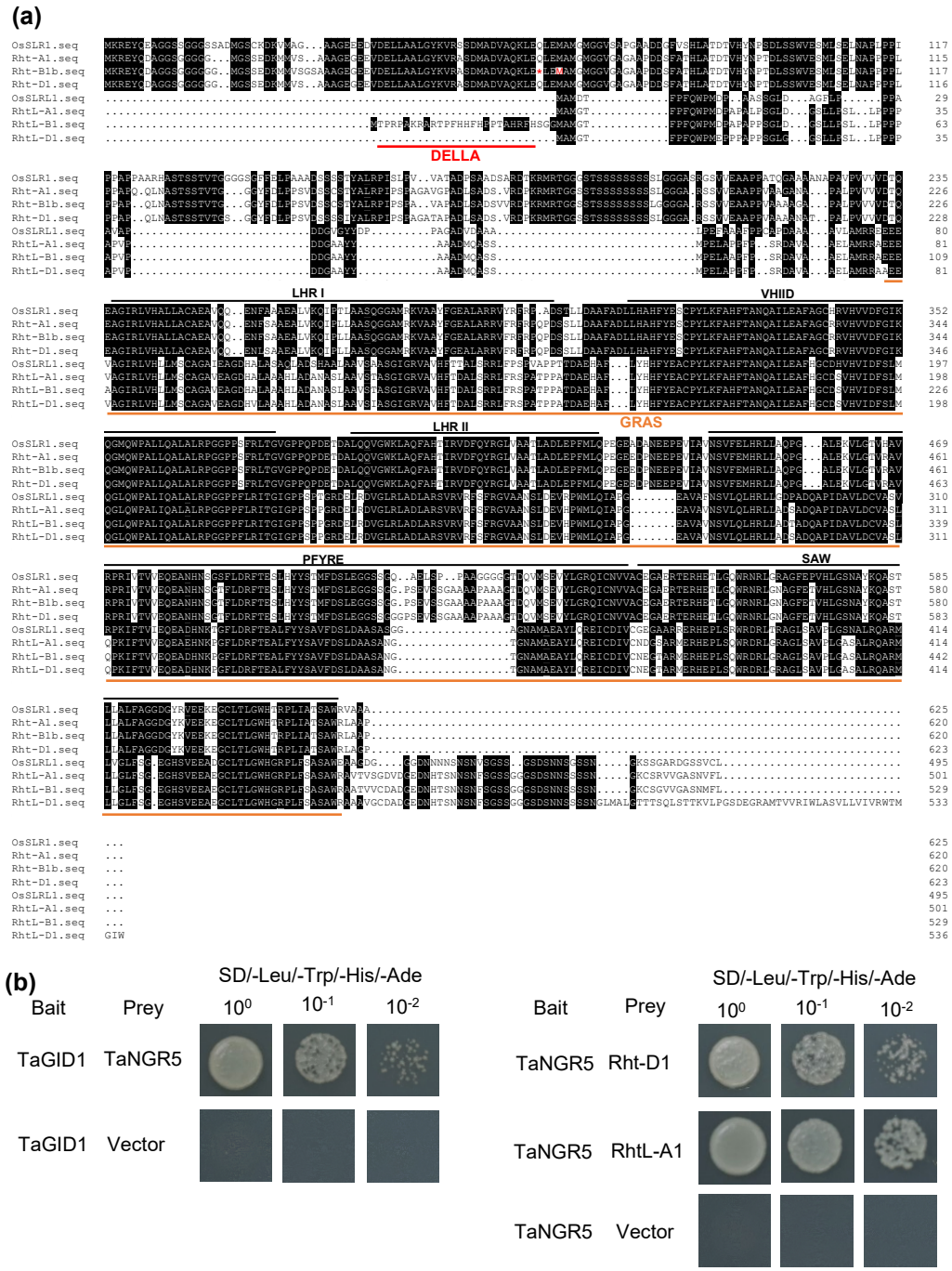

Figure S15 Sequence similarity of wheat and rice DELLA and DELLA-like proteins and their protein-protein interaction patterns showing their functional conservation. (a) Multiple alignment of the three homoeologs of wheat Rht-1 and RhtL1 and the rice SLR1 and SLRL1 proteins. The red line indicated the DELLA domain, and the orange line highlighted the GRAS domain. The black lines above the alignment indicated the conserved regions in the GRAS proteins. The red asterisk represented the stop codon position in *Rht-B1b*. (b) Yeast two hybrid assays confirming the conservation of protein-protein interaction patterns of GID1, Rht1, RhtL1 and NGR5 in wheat. Yeast cells growing on selective media without Trp, Leu, His and Ade indicate positive interactions.

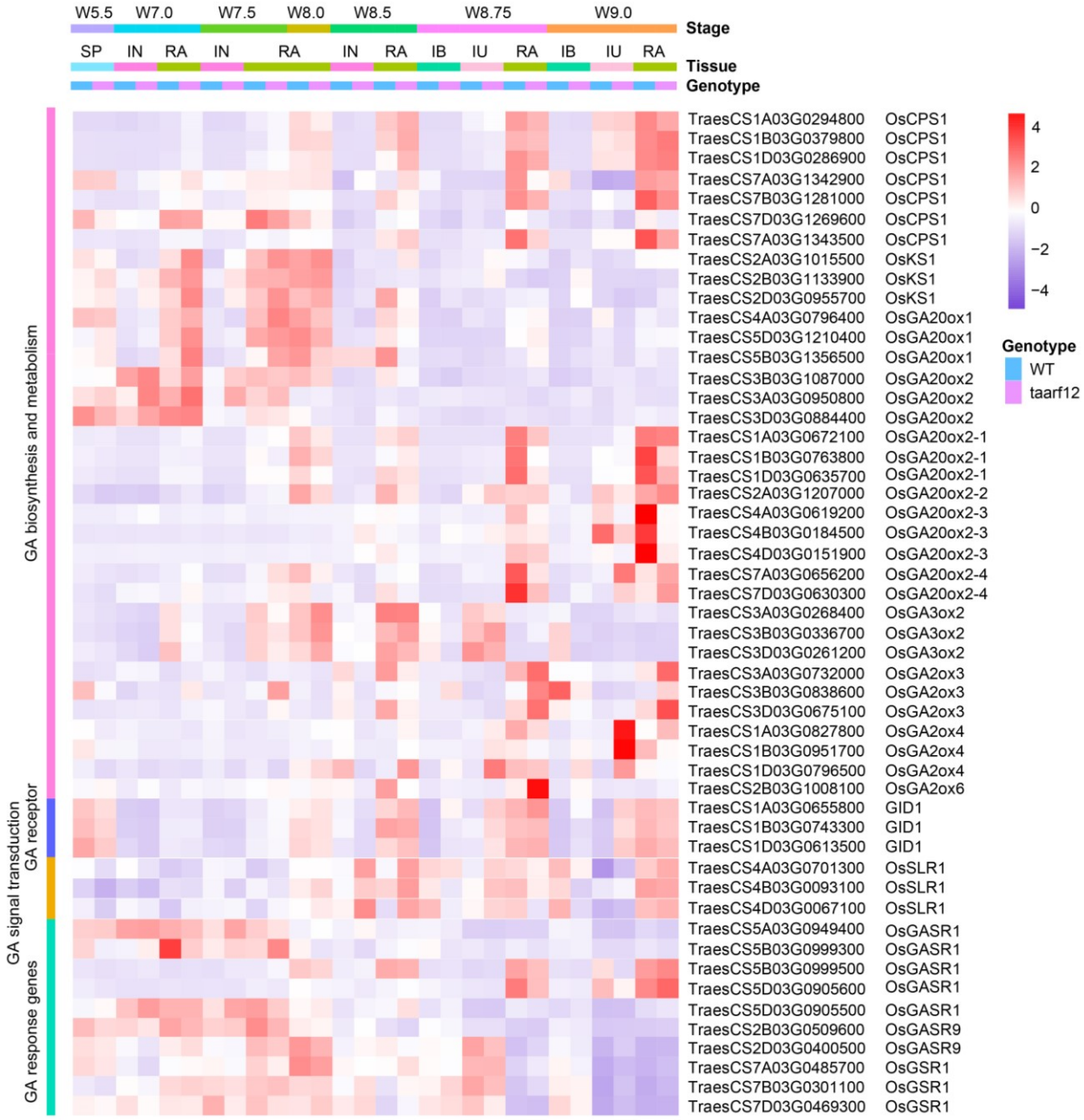

Figure S16 Heatmap showing spatial-temporal expression patterns of DEGs in the GA pathway. IB, internode bottom portion; IN, internode/peduncle; IU, internode upper portion; RA, rachis; SP, spike.

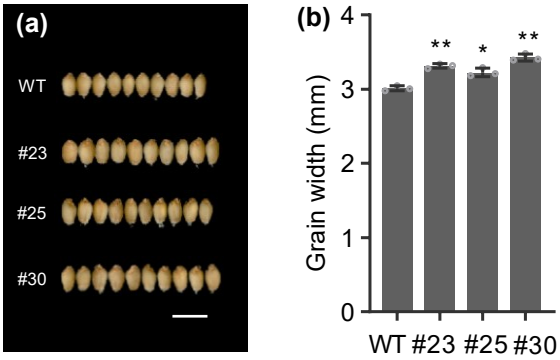

Figure S17 *TaNGR5* overexpression led to wider grains. (a) Over-expression of *TaNGR5* increased grain width relative to those of the wild type (WT) Fielder. Scale bar, 1 cm. (b) Statistical analysis of grain width in WT and over-expression of *TaNGR5* plants. Data were presented as mean ± s.d.; *P* values were determined by two-tailed Student's *t*-test. **P*< 0.05; ***P*< 0.01.

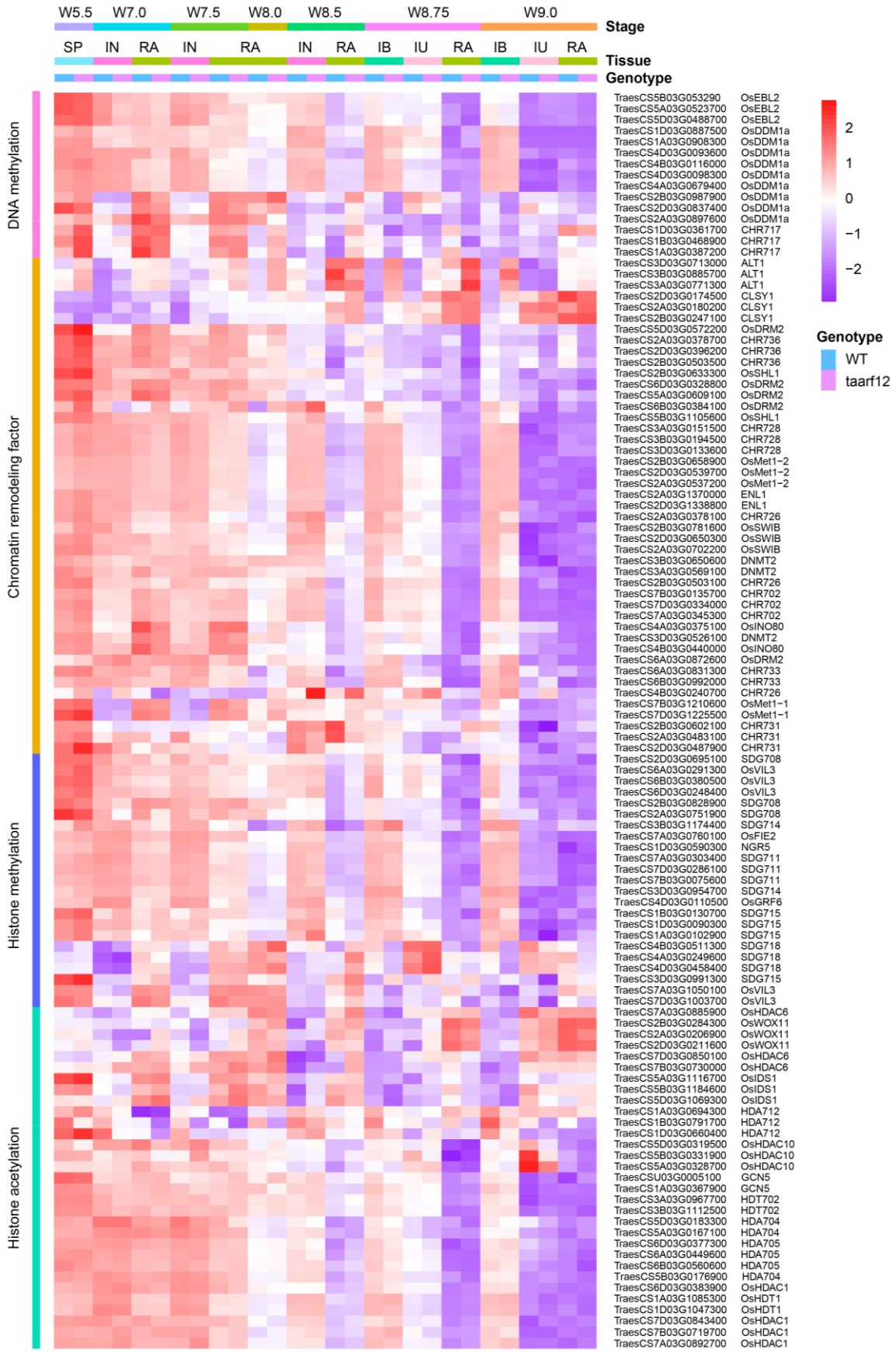

Figure S18 Heatmap showing spatial-temporal expression patterns of DEGs related to epigenetic modification. IB, internode bottom portion; IN, internode/peduncle; IU, internode upper portion; RA, rachis; SP, spike.

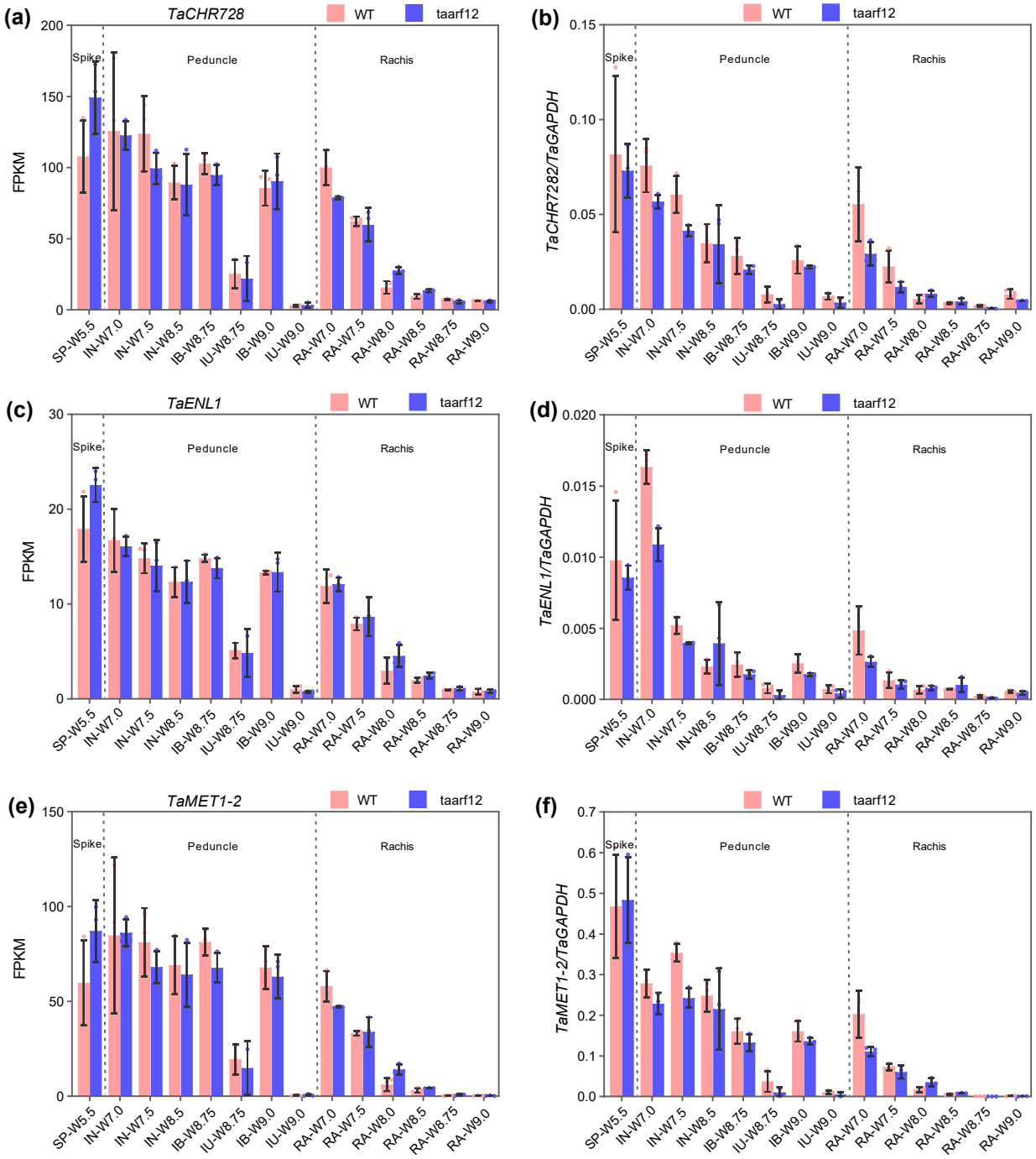

Figure S19 Confirmation of expression patterns of epigenetic modification genes in the wild type and *taarf12* plants. (a, c, e) Relative expression of epigenetic modification genes from RNA-seq data. (b, d, f) qRT-PCR analyses of epigenetic modification genes in wild type (WT) Fielder and *taarf12*. IB, internode bottom portion; IN, internode/peduncle; IU, internode upper portion; RA, rachis; SP, spike.

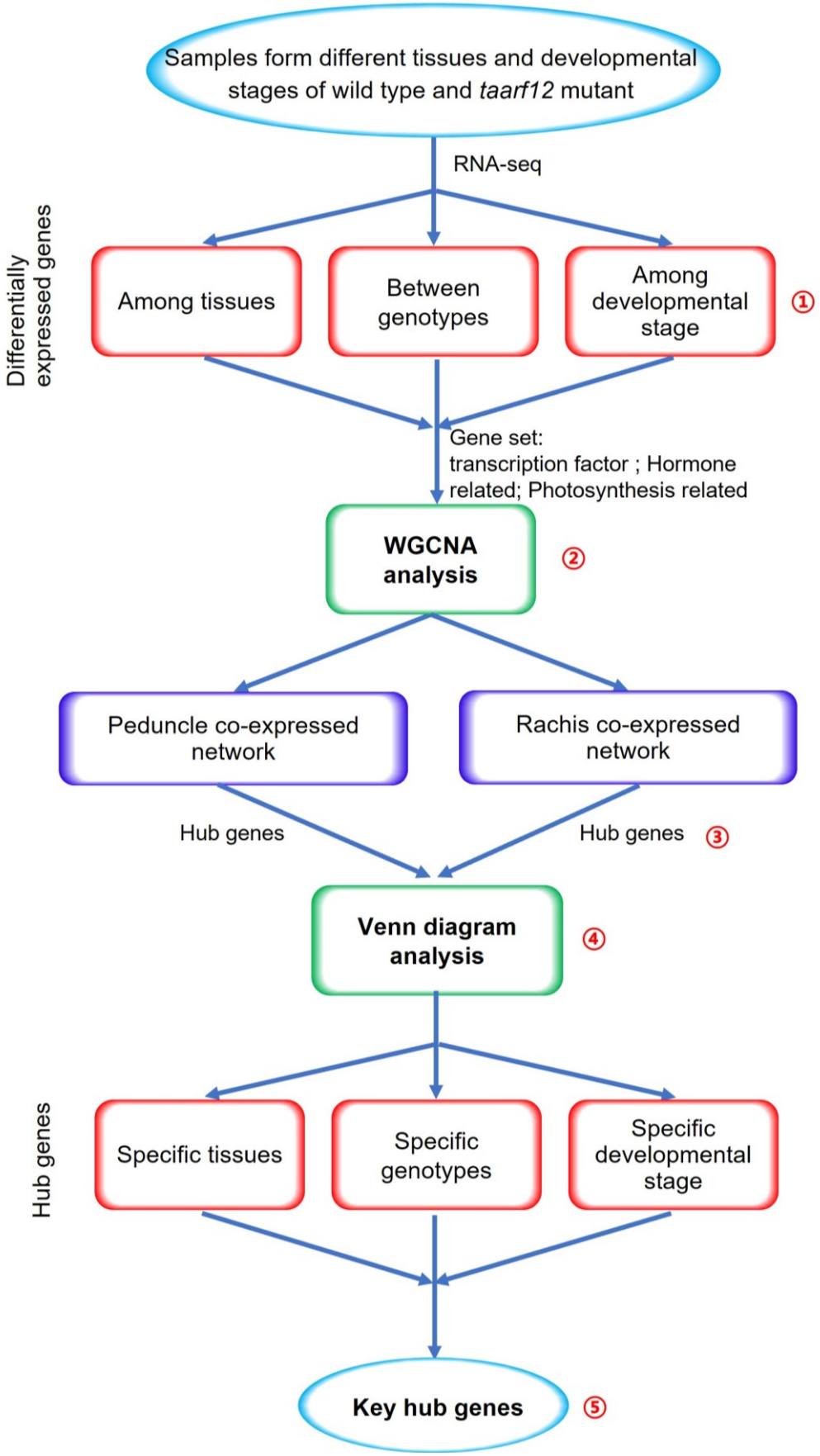

Figure S20 The RNA-seq analysis pipeline.